coefficients) as being accurate to not better than ±0.004. Jakli and Van Hook *(4)* have recently published the osmotic coefficients of, among other salts, calcium chloride as a function of temperature. Their extrapolated values at 0° agree with mine to within 0.004 at all concentrations up to 7*m*.

It is often useful to know the water activity of a saturated solution at some given temperature. The water activities of saturated solutions of the compounds studied here are given in Table III, along with their approximate concentrations.

Literature Cited

(1) Childs, C. W., Platford, R. F., *Aust. J. Chem.*, **24**, 2487 (1971).
(2) Glauque, W. F., Hornung, E. W., Kunzler, J. E., Rubin, T. R., *J. Amer. Chem. Soc.*, **82**, 62 (1960).
(3) Glueckauf, E., Kitt, G. P., *Trans. Faraday Soc.*, **52**, 1074 (1956).
(4) Jakli, G., Van Hook, W. A., *J. Chem. Eng. Data*, **17**, 348 (1972).
(5) Robinson, R. A., Stokes, R. H., "Electrolyte Solutions," p. 477, Butterworths, London, 1965.
(6) Scatchard, G., Prentiss, S. S., *J. Amer. Chem. Soc.*, **55**, 4355 (1933).
(7) Stokes, R. H., *Aust. J. Chem.*, **20**, 2087 (1967).
(8) Stokes, R. H., *J. Phys. Chem.*, **70**, 1199 (1966).

Received for review October 3, 1972. Accepted January 8, 1973.

Potassium Sulfate Crystal Growth Rates in Aqueous Solution

John W. Mullin[1] and Czeslaw Gaska

Department of Chemical Engineering, University College London, Torrington Place, London WC1E 7JE, United Kingdom

The growth kinetics of potassium sulfate crystals grown from aqueous solution at 20°C have been determined under carefully controlled conditions of temperature and supersaturation. The growth process is diffusion-controlled, being dependent on solution velocity up to about 140 mm/s, and shows an overall second-order dependence on supersaturation. However, the order changes from 2.0 for growth along the (001) crystallographic axis to 1.4 along the (100). Overall growth rates computed from the measured axial growth rates compare well with those measured in a multiparticle system in a fluidized bed crystallizer.

Potassium sulfate (mol wt = 174.26) crystallizes in the anhydrous form from aqueous solution as crystals belonging to the orthorhombic system. A common habit of this salt grown at low supersaturation is shown in Figure 1. The predominant crystallographic faces are (010) and (021).

The solubility of potassium sulfate in water over the temperature range $20 < \theta < 60$°C may be represented by the equation:

$$c^* = 0.067 + 0.0023\theta - 0.000006\theta^2 \qquad (1)$$

An empirical correlation *(6)* between diffusivity and viscosity over the temperature range $15 < \theta < 50$°C is:

$$D\eta \times 10^{13} = 8.1 + 0.071\theta \qquad (2)$$

where D = m²/s and η = N s/m². The activation energy of diffusion has been determined *(6)* as 20 kJ/mol.

Other relevant properties include: crystal density, ρ_c = 2660 kg/m³, density of saturated solution at 20°C, ρ_s = 1082 kg/m³, viscosity of saturated solution at 20°C, η_s = 1.2×10^{-3} N s/m².

Growth Rate Measurements

The growth rates of single crystals of potassium sulfate were measured by a technique previously described *(1, 2, 4)*. Briefly, a crystal was mounted on a wire in a glass cell, through which a solution flowed under carefully controlled conditions. Any chosen face or edge could be observed, with a traveling microscope reading ±0.01 mm, and its rate of advance measured. Solutions were prepared from recrystallized potassium sulfate and deionized water and filtered through a No. 4 (30 μm) sintered glass filter. Seed crystals were carefully selected from batches grown in a laboratory-scale fluidized bed crystallizer *(1, 5)* by hand picking from a close sieve cut (22/25 mesh BS, mean size 650 μm). Slightly elongated crystals with well-defined faces, free from inclusions and outgrowths were chosen. These crystals were then grown to a larger size (~3 mm long, 1 mm wide) in the fluidized bed crystallizer at 20°C using a low supersaturation ($\Delta c \sim 0.008$ kg K_2SO_4/kg H_2O; $S \sim 1.07$) to avoid the production of inclusions and irregular growths.

The seed crystal, fixed on the wire with its longest axis vertical, was dipped into deionized water to remove any surface impurities and then introduced into the cell when the solution temperature had achieved a constant value of 20°C. The circulation velocity was adjusted to the desired value. The washing process removed the sharp edges and corners from the crystal so a short period of time (at least 15 min) was allowed for the crystal to "heal" itself before growth rate measurements were commenced. In view of the fact that several crystallographic

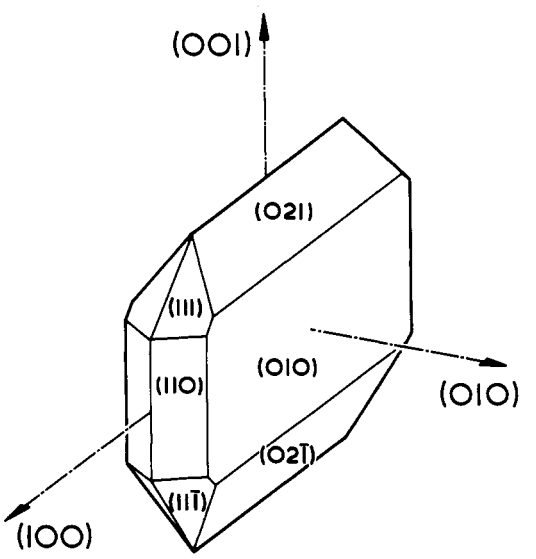

Figure 1. Typical habit of a potassium sulfate crystal grown from aqueous solution at low supersaturation

[1] To whom correspondence should be addressed.

faces were present (see Figure 1), it was decided to measure growth in two axial directions only.

The crystal was adjusted so that the maximum width was visible through the microscope. The increases in crystal width (001) and length (100) were measured at intervals of time. The duration of a run varied from about 1 to 4 hr depending on the solution supersaturation and velocity. Measurements were made at suitable regular intervals. At the end of a run, the final solution concentration was determined by a gravimetric technique, evaporating a filtered sample to dryness. The arithmetic mean concentration was taken as being representative of conditions during the growth process.

Effect of Solution Velocity. The effect of solution velocity between solution and crystal on the linear crystal growth rates in the (001) and (100) axial directions was measured at 20°C over the range 4 to 180 mm/s. It is important to note that this solution velocity in the glass cell was perpendicular to the (001) crystal axis and parallel to the (100). Figure 2 shows the (001) growth rates plotted against concentration driving force, Δc. For supersaturations of $\Delta c < 0.002$ no growth could be detected, but above this value the linear growth rate increased with Δc, slowly at first but more rapidly as Δc was increased. The growth rate also increased with solution velocity.

Similar results were recorded for the (100) axis growth rates, but the dependence of the (001) and (100) growth rates on the concentration driving force, Δc, are not the same (see Figure 3). If the data such as those in Figures 2 and 3 are plotted on logarithmic coordinates (not shown here) families of straight lines, of slope 2.0 for (001) and 1.4 for (100) are obtained. The linear growth rates can thus be related to the concentration driving force by an equation of the form:

$$v = k(\Delta c)^g \tag{3}$$

where g is the order of the growth process. The significance of this term is explained elsewhere *(1)*. For the two directions of growth the data give:

$$v_{(001)} = k_{(001)}(\Delta c)^{2.0} \tag{4}$$

and

$$v_{(100)} = k_{(100)}(\Delta c)^{1.4} \tag{5}$$

A similar situation has been recorded for the growth of ammonium sulfate crystals *(3)* where the (001) faces grow at a second-order rate and the (100) faces at a first-order.

The effect of solution velocity on the growth rates of potassium sulfate crystals in the (001) and (100) directions is seen more clearly in Figure 4. In both cases the growth rates increase with an increase in solution velocity up to about 140 mm/s after which further increases in velocity have no effect. This dependence of growth rate on solution velocity is indicative of a diffusion-controlled growth process *(1)*.

The (001) and (100) axial growth rates plotted in Figure 3 for solution velocities above the critical velocity of 140 mm/s show that for low concentration driving forces, $v_{(100)} > v_{(001)}$, but for $\Delta c > 0.008$ kg K_2SO_4/kg H_2O the reverse is the case. Thus, at high supersaturations granular (equidimensional) crystals should be obtained, and at low supersaturations (i.e., Δc, < 0.008 kg K_2SO_4/kg H_2O) elongated crystals may be expected.

A similar situation was recorded for solution velocities lower than the critical velocity of 140 mm/s, but it is interesting to note that crossover in growth rates occurs at lower values of Δc. For example, at a velocity of 4 mm/s the crossover occurred at $\Delta c = 0.008$ kg K_2SO_4/kg H_2O. The difference in growth rates along the (001) and (100) axes is also much less at the low solution velocity of 4 mm/s at equivalent concentration driving forces. There is, therefore, a complex dependence of crystal habit on supersaturation and solution velocity. For example, the results suggest that large crystals, which would have high relative solid–solution velocities in a fluidized bed crystallizer, should tend to grow in a granular form. In general, this is so *(5)*.

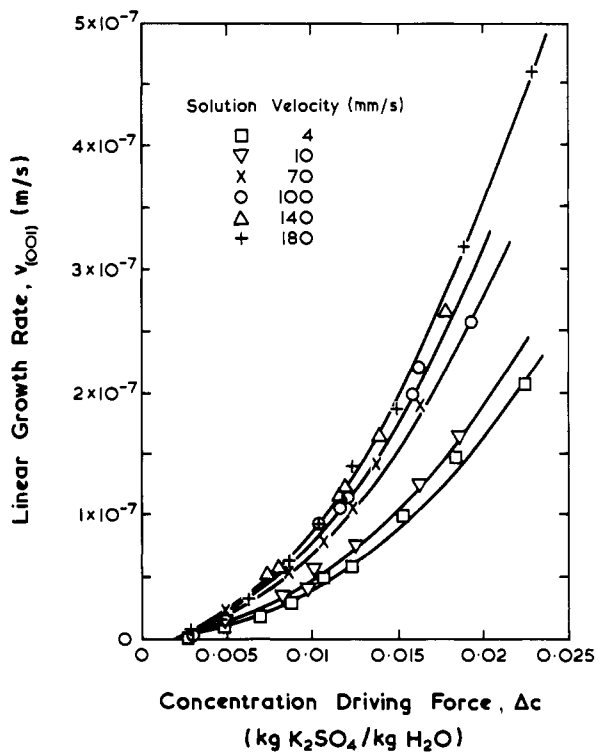

Figure 2. Effect of supersaturation and solution velocity on the (001) axis linear growth rate of potassium sulfate at 20°C

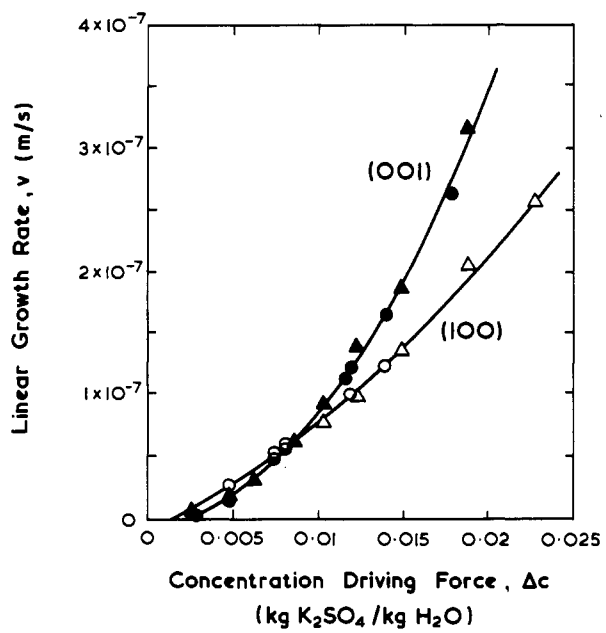

Figure 3. Comparison of (001) and (100) axial growth rates at 20°C at solution velocities of 140 [○ and ●] and 180 mm/s [△ and ▲], respectively

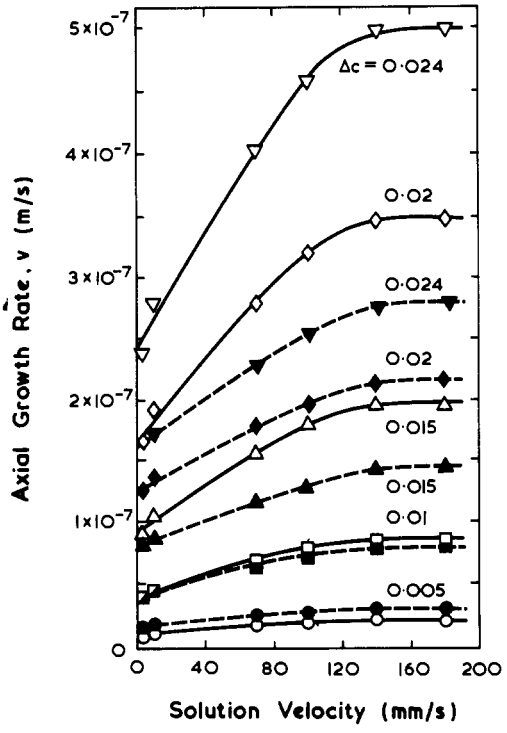

Figure 4. Effect of supersaturation and solution velocity on the (001) and (100) axial growth rates of potassium sulfate at 20°C, showing a critical velocity of about 140 mm/s

Open symbols refer to (001) and black symbols to (100)

Comparison of Linear Growth Rates

Overall crystal growth rates for crystals grown in a fluidized bed crystallizer may be determined by growing a known mass and size distribution of seeds under carefully controlled conditions. The mass deposition on crystals in selected size ranges, determined by sieving, is expressed in terms of a relationship of the form

$$R_G = \frac{1}{A} \cdot \frac{dm}{dt} = K_G(\Delta c)^g \qquad (6)$$

If we assume the crystals to be equivalent spheres, a mean overall equivalent linear growth rate may be expressed as

$$\bar{v} = \frac{R_G}{\rho_c} \qquad (7)$$

In general, clearly defined faces are not obtained on potassium sulfate crystals grown under these conditions; the crystals are usually opaque and rounded, so the above assumptions are reasonable.

Overall crystal growth rates, R_G, measured in a fluidized bed crystallizer on 0.4–1.6-mm crystals *(5)* show a second-order dependence on supersaturation—i.e., g = 2 in Equation 6. The linear growth rate $v_{(001)}$ measured in the cell on crystals up to 5 mm in size also shows a second-order dependence (Equation 4). Furthermore, both the overall and axial growth rates, R_G and $v_{(001)}$, increase with an increase in relative solid–solution velocity, the critical velocity in both cases being about 140 mm/s. It is interesting to note, however, that growth in the (100) direction is not second-order (Equation 5).

The overall growth rate R_G measured in the crystallizer, can be transformed into a mean linear growth rate $\bar{v}$ by dividing by the crystal density (Equation 7). However, linear growth rates thus calculated are not in very good agreement with linear growth rates measured in the growth cell. For example, the mean linear growth rate, $\bar{v}$, calculated *(5)* from R_G for Δc = 0.01 kg K_2SO_4/kg H_2O and a relative solid–solution velocity of 160 mm/s is 4.7 × 10^{-8} m/s. The linear growth rate $v_{(100)}$ measured in the cell under the same conditions of concentration driving force and solution velocity was 7.8 × 10^{-8} m/s (Figure 4).

Of course, these two types of growth rate are not strictly comparable, except for geometrically regular crystals such as cubes or octahedra. Linear growth rates measured in the cell correspond to an increase in one direction only [in the above case along the (100) axis] and this is not necessarily the same as that in another direction. The growth rate in the (001) direction, for example, under the same conditions is 8.6 × 10^{-8} m/s. On the other hand, the mean linear growth rate, $\bar{v}$, calculated from the mass transfer coefficient, R_G, is an overall average, which is not a very meaningful quantity for a thin elongated crystal such as that being considered above.

Comparison of Mass Transfer Rates

Another way to compare the different types of crystal growth rate is to estimate the mass transfer coefficient from the linear velocities, as measured in the growth cell, and to compare this coefficient with the overall value measured on crystals in the fluidized bed crystallizer.

For this purpose the crystal dimensions will be taken to be the same as the seed crystals used in the single crystal growth cell. The crystal will be assumed to be a parallelepiped, of width (001) and length (100) 1.5 and 3.5 mm, respectively. The thickness of the crystal (010) was approximately half the width, so a value of 0.75 mm will be used.

For growth at 20°C, a relative solid–solution velocity of 160 mm/s and a concentration driving force, Δc, of 0.01 kg K_2SO_4/kg H_2O the linear growth rate in the (001) and (100) directions are 8.6 × 10^{-8} and 7.8 × 10^{-8} m/s, respectively (Figure 4). Although the linear growth rate along the (010) axis was not measured, it probably had a growth rate of about half that for the (001) axis since during the growth of hand-picked seed crystals in the crystallizer (at 20°C and $\Delta c \sim$ 0.008 kg K_2SO_4/kg H_2O), the increase in crystal width to thickness was by a factor of about 2. The (010) growth rate was therefore assumed, for calculation purposes, to be 4.3 × 10^{-8} m/s.

Calculations may be made for other values of Δc giving a mean overall mass transfer coefficient, K_G, of 1.48 kg/s m^2 $(\Delta c)^2$ which compares well with the value of 1.28 measured in the fluidized bed crystallizer under comparable conditions *(5)*.

Nomenclature

A = crystal area, m^2
c = solution concentration, kg K_2SO_4/kg H_2O
c^* = equilibrium saturation concentration, kg K_2SO_4/kg H_2O
Δc = supersaturation ($c - c^*$) kg K_2SO_4/kg H_2O
D = diffusivity, m^2/s
g = order of crystal growth process (Equation 6)
k = linear growth rate constant (Equation 3)
K_G = overall mass transfer coefficient, kg/s m^2 $(\Delta c)^g$
m = mass, kg
R_G = overall crystal growth rate, kg/s m^2
S = supersaturation ratio, c/c^*
t = time, s
u = solution velocity, m/s

v = linear crystal growth rate, m/s
$\bar{v}$ = mean overall linear growth rate, m/s
η = viscosity (N s/m^2) 1 cP = 10^{-3} N s/m^2
η_s = viscosity of saturated solution, N s/m^2
θ = temperature, °C
ρ_c = crystal density, kg/m^3
ρ_s = density of saturated solution, kg/m^3

Subscripts (100) and (001) refer to the (100) and (001) crystal axes, respectively.

Literature Cited

(1) Mullin, J. W., "Crystallization," 2nd ed. pp 174–207, Butterworths, London, 1972
(2) Mullin, J. W., Amatavivadhana, A., *J. Appl. Chem. Lond.*, **17**, 151 (1967).
(3) Mullin, J. W., Chakraborty, M., Mehta, K., *J. Appl. Chem. Lond.*, **20**, 367 (1971).
(4) Mullin, J. W., Garside, J., *Trans. Inst. Chem. Engrs., Lond.*, **45**, 285 (1969).
(5) Mullin, J. W., Gaska, C., *Canad. J. Chem. Eng.*, **47**, 483 (1969).
(6) Mullin, J. W., Nienow, A. W., *J. Chem. Eng. Data*, **9**, 526 (1964).

Received for review October 12, 1972. Accepted January 18, 1973.

Conductivities and Densities of Aqueous Solutions of Quaternary Ammonium Iodides Containing Pentyl and Ethoxyethyl Groups

Barrie M. Lowe,[1] Neil A. MacGilp, and Jennifer M. Prichard

Department of Chemistry, University of Edinburgh, Kings Buildings, West Mains Road, Edinburgh EH9 3JJ, Scotland

The conductivities and densities of dilute aqueous solutions of the salts $R_3NR'I$ (R′ = pentyl or ethoxyethyl, R = Me or Et) have been measured at 25°C. Analysis of the molar conductivities with the Fuoss-Hsia and Pitts equations shows that all four salts form ion pairs and that the association constants of the ethoxyethyl compounds are lower than those of their pentyl analogs. The higher limiting molar ionic conductivities observed for the ethoxyethyl salts are correlated with their smaller volumes.

In a previous investigation *(10)* it was shown that the limiting molar conductivities of small quaternary ammonium iodides depend primarily on the size rather than the shape of the cation, and it was also shown that these salts form ion pairs to an extent which increases with increasing cation size. The purpose of the work reported here was to establish whether these relationships still hold when a methylene group in the cation is replaced by an ether oxygen.

Conductance measurements were made at 25°C on aqueous solutions of the iodides of pentyltrimethylammonium, ethoxyethyltrimethylammonium, pentyltriethylammonium, and ethoxyethyltriethylammonium cations, and their densities *(1)* were redetermined with a commercial density meter.

Experimental

The apparatus and procedure for the conductance measurements have been described *(10)*. The cell was rebuilt and had a cell constant of 0.48644 cm^{-1}, determined with potassium chloride solutions for which resistances were calculated using the equation of Lind et al. *(9)*. The solvent conductivity was allowed for. Temperature fluctuations in the oil thermostat bath did not exceed ±0.01°C.

Densities of solutions with concentrations in the range 0.02–0.2 mol kg^{-1} were measured with an Anton Parr DMA 02C density meter. The sample temperature was controlled to ±0.05°C with a Haake-type FE thermostat. The density meter was calibrated daily with at least three sodium chloride solutions with molalities in the range 0–0.9 mol kg^{-1}. The densities of these solutions were calculated from the equation,

$$d = 0.997046 + 0.0416600m - 0.0014972m^{3/2} - 0.0009876m^2 \quad (1)$$

which is based on densities calculated from the smoothed apparent molal volumes [The value of ϕ_v° for m = 0.3 mol kg^{-1} is 17.62(1) cm^3 mol^{-1} *(18)*] for $m \leq$ 0.9 mol kg^{-1} of Vaslow *(17)*. It represents these densities to within 1.4 × 10^{-6} g cm^{-3} and those of Millero *(12)* for $m \leq$ 0.51 mol kg^{-1} to within 12 × 10^{-6} g cm^{-3}. All solutions were prepared with boiled distilled water, and vacuum corrections were applied to all weights. The procedure was tested with potassium chloride solutions and the apparent molal volume derived from these measurements was 26.8(2) ± 0.2 (standard error) cm^3 mol^{-1} which is in excellent agreement with the literature *(13)* values (26.8 − 26.9 cm^3 mol^{-1}).

The salts were prepared and purified as described previously *(1)* and were dried in vacuo at 100°C for at least 24 hr before use. All samples had analyses for iodide which showed that they were at least as pure as those used in earlier work *(1)*.

Results

The experimental errors in the density measurements arise from the uncertainty in the sample temperature (±0.05°C) and from the solution handling procedures. The maximum error in the values given in Table I is estimated to be 3 × 10^{-5} g cm^{-3}. The densities can be represented to within this experimental error by the empirical equation

$$d = d_0 + a_1m + a_2m^2 \quad (2)$$

in which d_0 is the density of pure water (0.997046 g cm^{-3}) and a_1 and a_2 have the values given in Table II. The molarities, c, calculated from the observed densities are related to the molalities, m, by the equation

$$c = m(d_0 + A_1m + A_2m^2) \quad (3)$$

in which A_1 and A_2 are empirical constants given in Table II. The apparent molal volumes ϕ_v calculated from the observed densities were fitted to the equation *(1, 2)*

$$\phi_v = \phi_v^\circ + S_vc^{1/2} + jc \quad (4)$$

[1] To whom correspondence should be addressed.